Lecture 2. Measurements with contact in heat transfer: principles, implementation and pitfalls

F Lanzetta[1], B Garnier[2]

[1] FEMTO-ST, UMR CNRS 6174, Energy Department, Univ. Bourgogne Franche-Comté, Belfort, France
E-mail: francois.lanzetta@univ-fcomte.fr

[2] Laboratoire de Thermique et Energie de Nantes, UMR CNRS 6607, Univ. Nantes, France
E-mail: bertrand.garnier@univ-nantes.fr

Abstract. The main objective of this lecture is to make the end users aware of the various physical phenomena and especially of the errors frequently met during temperature and heat flow measurement. The lecture is divided in two main parts dealing with thermal measurement at macroscale, micro and nanoscales respectively. In Part 1, phenomena which occur in thermometry with contact (thermoelectric effects, thermoresistance) will be presented. For thermometry with contact, the analysis of systematic errors related to the local disturbance of field temperature due to the introduction of sensors will be emphasized. Indeed, intrusive effects due to sensors are usually ignored and can be reduced using know how as will be shown through analytical modeling. Otherwise, interests of using semi-intrinsic thermocouples will be discussed. The specificities of temperature measurement in fluid flow will be detailed. Finally heat flow measurement using direct methods (gradient, enthalpic, electric dissipation …) or inverse methods (heat flow sensors with network of thermocouples) will be reminded.

1. Introduction: General notions about temperature sensors

Mediums are in interaction with the environment, the interaction can be of several types: thermal, electrical, magnetic, liquid or vapor mass transfer, chemical reaction, corrosion … The installation of sensor on or inside the mediums should not modify these interactions. The choice of the sensor is performed so that these interactions do not have an effect on the measurement and on the lifespan of the sensor. For example, a sensor placed on the surface of a medium, can modify heat transfer by conduction, convection or radiation. Otherwise, the deposit of a liquid film or a coating modifies emissivity and therefore the radiative heat exchanges. The main consequence is that the temperature provided by the sensor can be very different from the one to measure. One important thing to keep in mind, is that temperature measurement is accompanied by parasitic effects which must be well-known. According to the type of interaction between sensor and medium, one can classify the methods of measurement in three categories:

1. *Methods with direct contact sensor-medium:* in this type of method, the sensor tends to locally equilibrate itself with the medium. If there is perfect adiabaticity of the sensor with the environment, its temperature is equal to that of the medium. However, in thermometric devices, this adiabaticity is usually not perfect.
2. *Methods with contact without physical connection with the environment*: in some cases, the temperature readings are carried out using an optical mean therefore no physical connection exists between the sensor and the environment. In this category, we can find surface temperature measurement with deposited thermosensitive material such as liquid crystals or photoluminescent salts.

3. *Methods without contact*: in this method sensors are far from the medium. Despite there is still interactions between them, the sensor is no more in equilibrium with the medium. Such methods are essentially based on radiative heat transfer.

In this lecture, one will discuss temperature measurement with contact. A focusing on the main methods (thermoelectric, thermoresistance) will be performed. First of all, temperature measurement using thermoelectric effects will be analyzed in various situations (temperature measurement in fluids, in semi-transparent medium and in opaque medium). Then, recent progress for thermal measurement at micro and nanoscales using Scanning Thermal Microscopy (STM) methods will be presented.

2. Phenomena and sensors for temperature measurement

2.1. Thermoresistances

2.1.1. Metallic probes

They are commonly called Resistance Temperature Detectors (RTD). The thermosensitive parameter in these sensors is the electrical resistance varying with the empirical law such as:

$$R = R_0 [1 + \alpha (T - T_0) + \beta (T - T_0)^2] \quad (2.1)$$

Their respective sensitivities, α, are about 10^{-3} K^{-1} that is rather weak, but their accuracy is rather large and higher than that of the thermocouples (Table 2.1.). In the specified temperature range, their stability is good. The resistor probes have an almost linear answer. A resistance measurement device or a power supply with a low voltage voltmeter has to be used inducing a current about a few mA through the thermoresistive probes. One has to take care about self-heating or Joule effect in order to limit temperature bias. For practical applications, the thermoresistive probes are composed of a metallic layer deposited on a flat electrical insulating substrate (epoxy resin, ceramic, mica…) or cylindrical (glass, pyrex….). The size and the shape of these thermoresistive probes make them useful for average temperature measurement. In addition, their time constant is much larger than that of thermocouples due to their insulating substrate. Therefore, they will be used preferentially for temperature measurement in stationary mode.

Table 2.1. Characteristics of the main thermoresistive metallic probes

Metal	Sensitivity α (K^{-1})	Temperature range (°C)
Platinum	$4\ 10^{-3}$	-200 à +1000
nickel	$6\ 10^{-3}$	-190 à +350*
Copper	$4\ 10^{-3}$	-190 à +150**

*358°C=Curie point for Nickel (magnetic transformation)
**risk of oxydation for copper

2.1.2. Thermistors

The thermistors which are probes with semiconducting material are much more sensitive than the metallic probes (sensitivity 10 times larger), but they are less stable, and their calibration curve is strongly nonlinear:

$$R = R_0 \exp [B (1/T - 1/T_0)] \quad (2.2)$$

The thermistors are presented in several shapes: pearl, disc or rod. The pearls are made of semiconducting material dropped on two connecting wires. Their diameter is about 0.15 to 2.5mm. They can be coated with glass. The flat discs are of more important size (2 to 25 mm in diameter and 0.5 to

12 mm thick). The rods are metalized at their extremity for the contact with the connecting wires. Their time constant ranges from a few seconds to several tens of seconds and the temperature range for thermistors goes usually from -50°C to 500°C.

2.2. Thermoelectric effects: theory and practice

The thermocouple is the most widely electrical sensor in thermometry and it appears to be the simplest of electrical transducers. Thermocouples are inexpensive, small in size, rugged, and remarkably accurate when used with an understanding of their peculiarities. Accurate temperature measurements are typically important in many scientific fields for the control, the performance and the operation of many engineering processes. A simple thermocouple is a device which converts thermal energy to electric energy. Its operation is based upon the findings of Seebeck [1]. When two different metals *A* and *B* form a closed electric circuit and their junctions are kept at different temperatures T_1 and T_2 (Figure 2.1), a small electric current appears.

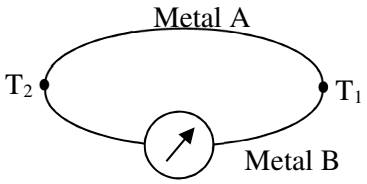

Figure 2.1. Thermocouple circuit.

The electromotive force, EMF, produced under these conditions is called the Seebeck emf. The amount of electric energy produced is used to measure temperature. The electromotive force depends on materials used in the couple and the temperature difference T_1-T_2. Seebeck effect is actually the combined result of two other phenomena, Peltier effect [2] and Thomson effect [3]. Peltier discovered that temperature gradients along conductors in a circuit generate an emf. Thomson observed the existence of an EMF due to the contact of two dissimilar metals and related to the junction temperature. Thomson effect is normally much smaller in magnitude than the Peltier effect and can be minimized and disregarded with proper thermocouple design.

a) Peltier effect

A Peltier electromotive force $V_M - V_N$ is created at the junction of two different materials (wire or film) A and B, at the same temperature *T,* depending on the material and the temperature *T* (Figure 2.2.):

$$V_M - V_N = \Pi_{AB}^T \tag{2.3}$$

Π_{AB} is the Peltier coefficient at temperature *T*.

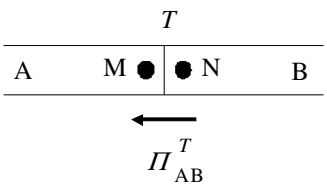

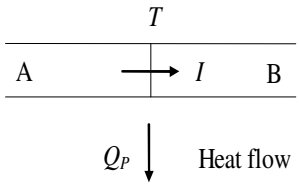

Figure 2.2. Peltier effect without current flow. **Figure 2.3.** Peltier effect with current flow.When a current *I* flows through a thermocouple junction (Figure 2.3.), heat, Q_P, is either absorbed or dissipated depending on the direction of current. This effect is independent of Joule heating.

$$dQ_P = (V_M - V_N)Idt = \Pi_{AB}^T Idt \tag{2.4}$$

Q_p is the heat quantity exchanged with the external environment to maintain the junction at the constant temperature T.
The phenomena are reversible, depending on the direction of the current flow and:

$$\Pi_{AB}^{T} = -\Pi_{BA}^{T} \tag{2.5}$$

b) Volta's law

In an isothermal circuit composed by different materials, the sum of the Peltier EMFs is null (Figure 2.4.) and:

$$\Pi_{AB} + \Pi_{BC} + \Pi_{CD} + \Pi_{DA} = 0 \tag{2.6}$$

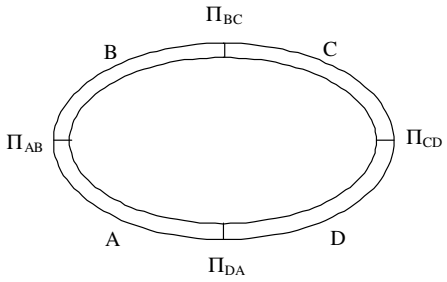

Figure 2.4. Volta's law with four materials.

c) Thomson effect

Thomson EMF's corresponds to the tension $e_A(T_1,T_2)$ between two points M and N of the same conductor, submitted to a temperature gradient, depending only on the nature of the conductor (Figure 2.5.):

$$e_A(T_1,T_2) = \int_{T_1}^{T_2} \tau_A dT \tag{2.7}$$

Where τ_A is the Thomson coefficient of the material A.

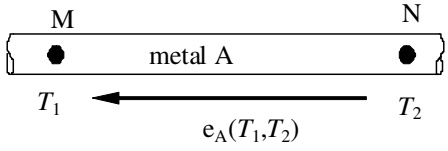

Figure 2.5. Thomson effect without current flow.

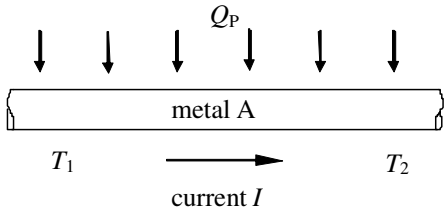

Figure 2.6. Thomson effect with current flow.

When a current I flows through a conductor within a thermal gradient ($T_1 - T_2$), heat Q_T, is either absorbed or dissipated (Figure 2.6.):

$$dQ_T = e_A(T_1,T_2)\, I\, dt = \int_{T_1}^{T_2} \tau_A dT\; I\, dt \tag{2.8}$$

d) Seebeck effect

When a circuit is formed by a junction of two different metals A and B and the junctions are held at two different temperatures, T_1 and T_2, a current I flows in the circuit caused by the difference in temperature between the two junctions (Figure 2.7.).

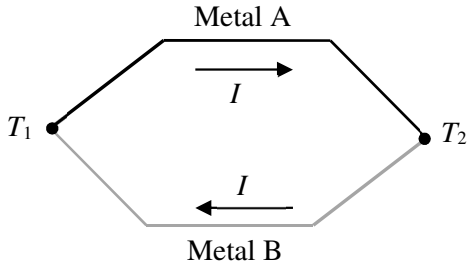

Figure 2.7. Seebeck effect.

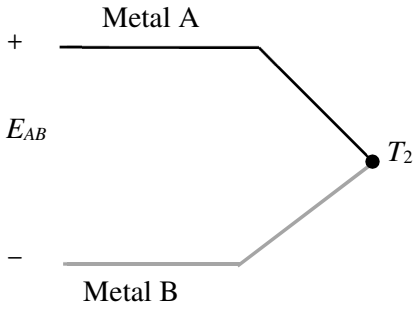

Figure 2.8. Seebeck Voltage.

The sum of the different Peltier and Thomson EMF for the circuit corresponds to the Seebeck EMF:

$$E_{AB}(T_2,T_1) = \Pi_{AB}^{T_1} + \Pi_{BA}^{T_2} + \int_{T_1}^{T_2} \tau_B dT + \int_{T_2}^{T_1} \tau_A dT$$
$$E_{AB}(T_2,T_1) = \Pi_{AB}^{T_1} - \Pi_{AB}^{T_2} + \int_{T_2}^{T_1} (\tau_A - \tau_B) dT \qquad (2.9)$$

Then, the Seebeck EMF becomes:

$$E_{AB}(T_1,T_2) = \sigma_{AB}(T_1 - T_2) \qquad (2.10)$$

σ_{AB} is the Seebeck coefficient for the A and B metals of the couple ($\mu V.°C^{-1}$ or $\mu V.K^{-1}$). This coefficient corresponds to a constant of proportionnality between the Seebeck voltage and the temperature difference.

If the circuit is open at the center of the circuit (Figure 2.8), the net open voltage is a function of the junction temperature and the composition of the two metals.

The thermoelectric power, or sensitivity, of a thermocouple is given by Table 2.2:

$$\sigma_{AB} = \frac{dE_{AB}}{dT} \qquad (2.11)$$

Table 2.2. Seebeck coefficients of various thermocouple materials relative to platinum at 0°C [4]

Material	Seebeck coefficient ($\mu V°C^{-1}$)	Material	Seebeck coefficient ($\mu V°C^{-1}$)
Bismuth	-72	Silver	6.5
Constantan	-35	Copper	6.5
Alumel	-17.3	Gold	6.5
Nickel	-15	Tungsten	7.5
Potassium	-9	Cadmium	7.5
Sodium	-2	Iron	18.5
Platinum	**0**	Chromel	21.7
Mercury	0.6	Nichrome	25
Carbon	3	Antimony	47
Aluminium	3.5	Germanium	300
Lead	4	Silicium	440
Tantalum	4.5	Tellurium	500
Rhodium	6	Selenium	900

Thermocouples are made by the association of dissimilar materials producing the biggest possible Seebeck. In industrial processes, the common thermocouples are presented in Table 2.3.

3. Temperature measurement in fluids

3.1. Mathematical modelling

Transient phenomena appear in many industrial processes and many researchers and engineers have been paying attention to the measurement of temperature fluctuations in turbulent reacting flows, compressible flows, boiling, cryogenic apparatus, fire environments, under the condition of simultaneous periodical variations of velocity, flow density, viscosity and thermal conduction in gas [7-14].

Table 2.3. Thermocouple Types [5]

Type	Metal A (+)	Metal B (-)	Temperature range	Seebeck coefficient α (µV/°C) at T°C	Standard error	Minimal error	Comments
B	Platinum-30% Rhodium	Platinum-6% Platinum	0°C to 1820°C	5.96 µV at 600°C	0.5%	0.25%	Idem R type (glass industry)
E	Nickel 10% Chromium	Copper-Nickel alloy (Constantan)	-270°C to 1000°C	58.67 µV at 0°C	1.7% to 0,5%	1% to 0.4%	Interesting sensitivity
J	Iron	Copper-Nickel alloy (Constantan)	-210°C to 1200°C	50.38 µV at 0°C	2.2% to 0.75%	1.1% to 0.4%	For atmosphere reduced (plastic industry)
K	Nickel-Chromium alloy (Chromel)	Nickel-Aluminium alloy (Alumel)	-270°C to 1372°C	39.45 µV at 0°C	2.2% to 0.75%	1.1% to 0.2%	The most widely used because of its wide temperature range, supports an oxidizing atmosphere
N	Nickel-Chromium-Silicium alloy (Nicrosil)	Nickel-Silicium alloy (Nisil)	-270°C to 1300°C	25.93 µV at 0°C	2.2% to 0.75%	1.1% to 0.4%	New combination very stable
R	Platinum-13% Rhodium	Platinum	-50°C to 1768°C	11.36 µV at 600°C	1.5% to 0.25%	0.6% to 0,1%	High temperature applications, resists oxidation
S	Platinum-10% Rhodium	Platinum	-50°C to 1768°C	10.21 µV at 600°C	1.5% to 0.25%	0.6% to 0.1%	Idem R type
T	Copper	Copper-Nickel alloy (Constantan)	-270°C to 400°C	38.75 µV at 0°C	1% to 0.75%	0.5% to 0.4%	Cryogenic applications
W	Tungsten	Tungsten-26% Rhenium	+20°C to +2300°C				Sensitive to oxidizing atmospheres, linear response and good performance in high temperature
W3	Tungsten-3% Rhenium	Tungsten-25% Rhenium	+20°C to +2000°C				Idem W type
W5	Tungsten-5% Rhenium	Tungsten-26% Rhenium	+20°C to +2300°C				Idem W type

There has been considerable progress in recent years in transient thermometry techniques. Some of these techniques are applicable for both solid material characterization while others are suitable only for fluids thermometry. This chapter deals only with temperature thermocouples measurements in fluids (gases and liquids). Many concepts involved in the temperature measurements in fluids are common to both types and they are discussed here. The techniques for temperature measurement in a fluid consists in inserting a thermocouple, allowing it to come to thermal equilibrium and measuring the generated electrical signal. When a thermocouple is submitted to a rapid temperature change, it will take some time to respond. If the sensor response time is slow compared to the change rate of of the measured

temperature,the thermocouple will not be able to faithfully represent the dynamic response of the temperature fluctuations. Then, the problem is to measure the true temperature of the fluid because a thermocouple gives only its own temperature. The temperature differences between the fluid and the sensor are also influenced by thermal transport processes taking place between the fluid to be measured, the temperature sensor, the environment and the location of the thermocouple. Consequently, the measured temperature values must be corrected. Whereas in steady conditions only the contributions of the conductive, convective and radiative heat exchanges with the external medium occur, unsteady behavior introduces another parameter which becomes predominant: the junction thermal lag which is strongly related to its heat capacity and thermal conductivity. The corrections generally decrease with the thermocouple diameters, and both temporal and spatial resolutions are improved. However, while spatial resolution is fairly directly connected with the thermocouple dimensions, the temporal resolution doesn't only depend on the dimensions and the thermocouple physical characteristics, but also on the rather complex heat balance of the whole thermocouple. To obtain the dynamic characteristics of any temperature probe, we analyze its response to an excitation step from which the corresponding first time constant τ can be defined as :

$$\tau = \frac{\rho\, c\, V}{h\, A} \tag{2.12}$$

τ is the time constant, ρ the density, c the specific heat, V the volume of the thermocouple and A the area of the fluid film surrounding the thermocouple while h is the heat transfer coefficient.

The goal of this work consists in calculating or measuring time constants of thermocouples and comparing their behavior according to different dynamical external heating like convective, radiative and pseudo-conductive excitations.

An accurate calibration method is an essential element of any quantitative thermometry technique, and the goal of any measurement is to correctly evaluate the difference between the "true" temperature and the sensor temperature. Figure 2.9. shows the energy balance performed at the butt-welded junction of a thermocouple for a junction element *dx* resulting from the thermal balance between the rate of heat stored by the junction $d\dot{Q}_{th}$ and heat transfer caused by:

- convection in the boundary layer around the thermocouple $d\dot{Q}_{cv}$
- conduction along the wires $d\dot{Q}_{cd}$
- radiation between the wires and the external medium $d\dot{Q}_{rad}$
- contribution of another source of heat power (a laser source in this example) $d\dot{Q}_{ext}$.

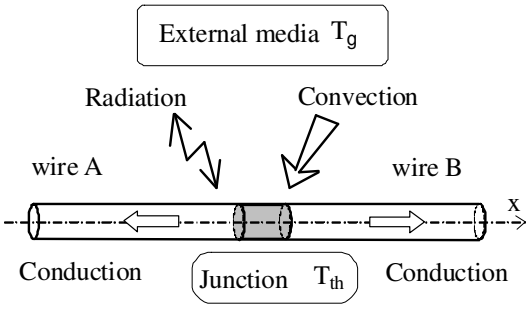

Figure 2.9. Heat balance for the probe

During a transient period, because of its thermal capacity, the thermocouple temperature will lag behind any gas temperature variation. This leads to an error from which a thermocouple time constant can be defined. The general heat balance for a junction of length *dx* is expressed as :

$$d\dot{Q}_{th} = d\dot{Q}_{cv} + d\dot{Q}_{cd} + d\dot{Q}_{rad} + d\dot{Q}_{ext} \tag{2.13}$$

The thermoelectric junction stores the heat by unit time $d\dot{Q}_{th}$:

$$d\dot{Q}_{th} = \rho_{th} c_{th} \frac{\pi d^2}{4} \frac{\partial T_{th}}{\partial t} dx \tag{2.14}$$

where ρ_{th}, c_{th} and T_{th} are the density, the specific heat and the temperature of the junction respectively. The junction is approximated by a cylinder whose diameter equals the wire diameter *d*. This does not exactly fit reality but remains currently used in numerical calculations [15-21]. Moreover, if the wires are uniformly curved, the observation near the junction confirms the previous assumption (Figures 3.20 and 3.21). The Newton's law of cooling is:

$$d\dot{Q}_{cv} = \pi \, dx \, Nu \, \lambda_g \left(T_g - T_{th} \right) \tag{2.15}$$

where λ_g and T_g are the thermal conductivity and the static temperature of the gas. The difficulty is to obtain an accurate relation between the Nusselt number *Nu* and the flow characteristics around the junction assumed as a cylinder [17, 22-25].

Indeed, such a thermocouple is surrounded by both a thermal and aerodynamic gradient which acts as a thermal resistance that is estimated from empiric approaches. A purely convective heat transfer coefficient *h* is generally deduced from correlations about the Nusselt number that is generally expressed as a combination of other dimensionless numbers, such as Eckert, Reynolds, Prandtl or Grashof numbers. However, if many cases have been investigated, the example of thin cylinders cooling process is still an open question. Table 2.4 gives a list of the main Nusselt correlations in this particular case.

Conduction heat transfer $d\dot{Q}_{cd}$ that occurs along the wires to the thermocouple supports has the following general expression:

$$d\dot{Q}_{cd} = \lambda_{th} \frac{\pi d^2}{4} \frac{\partial^2 T_{th}}{\partial x^2} dx \tag{2.16}$$

However, different studies and experiments have shown that conduction dissipation effects along cylindrical wires can be neglected when the aspect ratio between the length and the diameter is large enough [6, 26-32]. Indeed, practical cases of anemometry and thermometry have led to fix a condition such:

$$L/d > 100 \tag{2.17}$$

Hence, the temperature gradient can be considered null in the axial direction of the thermocouple wire. The thermocouple is placed in an enclosure at temperature T_w. The enclosure dimensions are assumed to be large with respect to the probe dimensions. Then, the influence of the radiative heat transfer can be expressed by the simplified form:

Table 2.4 Heat transfer laws – These laws describe the heat transfer from a cylinder of infinite length. The film temperature T_{film} is defined as the mean value between the fluid temperature T_f and the thermocouple temperature T_{th} [16-18, 20-25, 29-33]

Author	Temperature for λ, ρ and μ	Correlation	*Reynlod's number domain*
Andrews	T_f	$Nu = 0.34 + 0.65\,Re^{0.45}$	$0.015 < Re < 0.20$
Bradley and Mathews	T_f	$Nu = 0.435\,Pr^{0.25} + 0.53\,Pr^{0.33}\,Re^{0.52}$	$0.006 < Re < 0.05$ $0.7 < Pr < 1$
Churchill et Brier	T_f	$Nu = 0.535\,Re^{0.50}\left(T_f / T_{th}\right)^{0.12}$	$300 < Re < 2300$
Collis and Williams	T_{film}	$Nu = \left(0.24 + 0.56\,Re^{0.45}\right)\left(T_{film} / T_{gaz}\right)^{0.17}$	$0.02 < Re < 44$
Collis an Williams	T_{film}	$Nu = \left(0.48\,Re^{0.45}\right)\left(T_{film} / T_{gaz}\right)^{0.17}$	$44 < Re < 140$
Davies and Fisher	T_f	$Nu = \left(2.6/\gamma\pi\right)Re^{0.33}$	$0.01 < Re < 50$
Eckert and Soehngen	/	$Nu = 0.43 + 0.48\,Re^{0.5}$	$1 < Re < 4000$
Glawe and Johnson	T_f	$Nu = 0.428\,Re^{0.50}$	$400 < Re < 3000$
King	T_{film}	$Nu = 0.318 + 0.69\,Re^{0.5}$	$0.55 < Re < 55$
Kramers	T_{film}	$Nu = 0.42\,Pr^{0.2} + 0.57\,Pr^{0.33}\,Re^{0.5}$	$0.01 < Re < 10000$ $0.7 < Pr < 1000$
McAdams	T_{film} and T_f for ρ	$Nu = 0.32 + 0.43\,Re^{0.52}$	$40 < Re < 4000$
Olivari and Carbonaro	T_{film}	$Nu = 0.34 + 0.65\,Re^{0.45}$	$0.015 < Re < 20$ $L / d > 40$
Parnas	T_f	$Nu = 0.823\,Re^{0.5}\left(T_{th} / T_f\right)^{0.085}$	$10 < Re < 60$
Richardson	/	$Nu = 0.3737 + 0.37\,Re^{0.5} + 0.056\,Re^{0.66}$	$1 < Re < 10^5$
Scadron and Warshawski	T_f	$Nu = 0.431\,Re^{0.50}$	$250 < Re < 3000$
Van den Hegge Zijnen	T_{film}	$Nu = 0.38\,Pr^{0.2} + \left(0.56\,Re^{0.5} + 0.01\,Re\right)Pr^{0.33}$	$0.01 < Re < 10^4$

$$d\dot{Q}_{rad} = -\sigma\, \varepsilon(T_{th}) \left(T_{th}^4 - T_w^4\right) dS_{ray} \tag{2.18}$$

σ is the Stefan Boltzmann constant and $\varepsilon(T_{th})$ the emissivity of the wire at the temperature T_{th}. The exchange surface of the radiative heat transfer $dS_{rad} = \pi\, d\, dx$ is nearly equal to the surface exposed to the convective heat flux. This assumes that the radiative heat transfer between the sensor and the wall is greater than between the gas and the sensor. Here, the assumption is that the gas is transparent, however it is not satisfied in several practical applications like temperature measurements in flames.

In section 3.2.b, we will consider a radiative calibration so that the thermocouple junction is submitted to an external heat contribution $d\dot{Q}_{ext}$ produced by a laser beam [27].

$$d\dot{Q}_{ext} = \sqrt{\frac{2}{\pi}} \frac{\left(1-\bar{R}\right)}{a} P_L\, erf\left[\frac{d}{a\sqrt{2}}\right] exp\left[-2\frac{x^2}{a^2}\right] dx \tag{2.19}$$

P_L is the laser beam power, $\bar{R}$ the mean reflection coefficient of the thermocouple junction surface, d the diameter of the junction and a the laser beam radius (this value corresponds to the diameter for which one has *99 %* of the power of the laser beam).

The total heat balance of the thermocouple may be written as follows

$$\begin{aligned} &\rho_{th} c_{th} \frac{\pi d^2}{4} \frac{\partial T_{th}}{\partial t} = Nu\, \lambda_g \pi \left(T_g - T_{th}\right) + \lambda_{th} \frac{\pi\, d^2}{4} \frac{\partial^2 T_{th}}{\partial x^2} \\ &-\sigma\, \varepsilon(T_{th}) \left(T_{th}^4 - T_w^4\right) \pi\, d + \sqrt{\frac{2}{\pi}} \frac{\left(1-\bar{R}\right)}{a} P_L\, erf\left[\frac{d}{a\sqrt{2}}\right] exp\left[-2\frac{x^2}{a^2}\right] \end{aligned} \tag{2.20}$$

The expression of the gas temperature T_g is deduced from equation (2.20):

$$T_g = T_{th} + \tau_{cv} \left[\begin{array}{c} \dfrac{\partial T_{th}}{\partial t} - \dfrac{\lambda_{th}}{\rho_{th} c_{th}} \dfrac{\partial^2 T_{th}}{\partial x^2} + \dfrac{4\, \sigma\, \varepsilon(T_{th})}{\rho_{th} c_{th} d} \left(T_{th}^4 - T_w^4\right) \\ -\dfrac{4}{\rho_{th} c_{th} d^2} \sqrt{\dfrac{2}{\pi}} \dfrac{\left(1-\bar{R}\right)}{a} P_L\, erf\left[\dfrac{d}{a\sqrt{2}}\right] exp\left[-2\dfrac{x^2}{a^2}\right] \end{array} \right] \tag{2.21}$$

Equation 2.21 represents a general expression of the thermocouple dynamic behavior including each of the heat transfer modes. In this expression, the time constant τ_{cv} of the thermocouple junction is defined by:

$$\tau_{cv} = \frac{\rho_{th}\, c_{th}\, d^2}{4\, Nu\, \lambda_g} = \frac{\rho_{th}\, c_{th}\, d}{4\, h} \tag{2.22}$$

If the radiation, the conduction and the external heat supply are neglected, the gas temperature can be simplified by:

$$T_g = T_{th} + \tau_{cv} \frac{\partial T_{th}}{\partial t} \tag{2.23}$$

The time-response of a temperature sensor is then characterized by a simple first order equation. This is a common but erroneous way to do. For a step change in temperature, equation (2.23) reduces to:

$$\frac{T_g - T_{th}}{T_g - T_i} = exp\left[-\frac{t}{\tau_{cv}}\right] \tag{2.24}$$

where T_i is the initial temperature.

Conventionally, the time constant τ_{cv} is defined as the duration required for the sensor to exhibit a *63%* (= $1\text{-}e^{-1}$) change from an external temperature step, in the case of a single-order equationThe fact that different kinds of heat transfers are involved should lead to a global time-constant in which the different phenomena contributions are included [16, 29]. Consequently, the ability of a thermocouple to follow any modification of its thermal equilibrium is resulting from a multi-ordered time response where the most accessible experimental parameter remains the global time constant. The multi-ordered temperature response of a thermocouple can be represented by the general relation:

$$\frac{T_g - T_{th}}{T_g - T_i} = K_1\, exp\left[-\frac{t}{\tau_1}\right] - K_2\, exp\left[-\frac{t}{\tau_2}\right] - \cdots - K_n\, exp\left[-\frac{t}{\tau_n}\right] \tag{2.25}$$

T_i is the initial temperature, T_g is the fluid temperature. The value of the constants K_1, K_2, …, K_n as well as the time constants τ_1, τ_2, …, τ_n, depend on the heat flow pattern between the thermocouple and the surrounding fluid.

If experiments have shown that most configurations involve nearly first-order behaviors, the measured time-constant does not allow to isolate each of the different contribution modes.

Therefore, the remaining problem of experiments is to relate this global time-constant to the different implied heat transfer modes. Then, our contribution in this section will be to show the influence of the heat transfer condition on the measured time constant value through three different methods of dynamic calibration.

Classical testing of thermocouples often involves plunging them into a water or oil bath and for providing some information only about the response of the thermocouple under those particular conditions. It does not provide information about the sensor response under process operating conditions where the sensor is used. In order to improve thermocouple transient measurements, a better understanding of the dynamic characteristics of the sensor capability is necessary.

3.2. Dynamic calibration

The calibration methods consist of a series of heating and cooling histories performed by submitting the thermocouple to different excitation modes. Then, the resulting exponential rise and decay times of the thermocouple signals allow to estimate the time constant τ. The thermocouple signal is amplified with a low-noise amplifier having a –3 dB bandwidth of 25 kHz (Gain = 1000). The output voltage is finally recorded by a digital oscilloscope.

a) Convective calibration

Figure 2.10. illustrates the convective experimental device. The thermocouple junction is exposed continuously to a constant cold air-stream at constant temperature T_{MIN}. A second hot air flow excites periodically the thermocouple and creates a temperature fluctuation of frequency f [33].

The response of a thermocouple submitted to successive steps of heating or cooling is close to a classical exponential first order response from which the time constant can be determined (Figure 2.11.). It can be deduced from the measurement of four temperatures: T_{MAX}, T_{MIN}, $T_{th\,max}$ and $T_{th\,min}$.

For the heating period t_h, we define the temperature differences δ_{1h} and δ_{2h}:

$$\delta_{1h} = T_{MAX} - T_{th\,min} \quad \text{and} \quad \delta_{2h} = T_{MAX} - T_{th\,max} \qquad (2.26), (2.27)$$

For the cooling period t_c, the temperature differences δ_{1c} and δ_{2c} by:

$$\delta_{1c} = T_{th\,max} - T_{MIN} \quad \text{and} \quad \delta_{2c} = T_{th\,min} - T_{MIN} \qquad (2.28), (2.29)$$

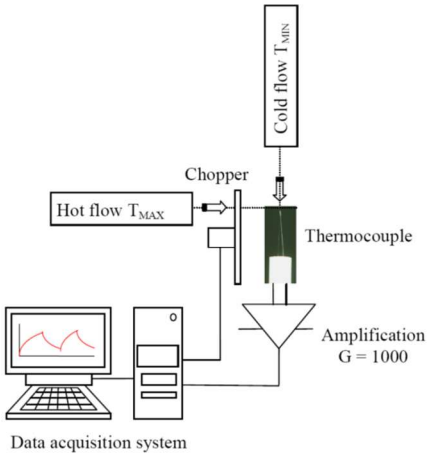

Figure 2.10. Convective characterization setup

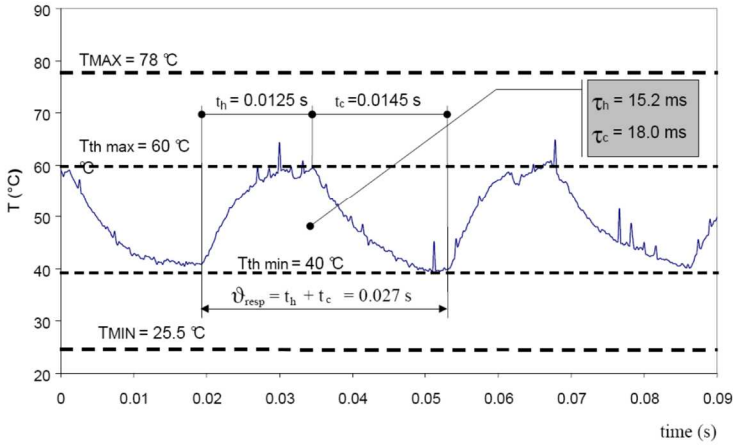

Figure 2.11. Convective characterization results

Then, the two convective time constants are defined while the thermocouple is heating (τ_h) and cooling (τ_c). If we consider a first order response of the sensor we obtain the expressions:

$$\tau_h = \frac{t_h}{ln(\delta_{1h}/\delta_{2h})} \text{ and } \tau_c = \frac{t_c}{ln(\delta_{1c}/\delta_{2c})} \qquad (2.30), (2.31)$$

Then the period of the thermocouple response is:

$$\vartheta_{resp} = t_c + t_h \qquad (2.32)$$

Figure 2.11 presents temperature histories for a 12.7 µm K type thermocouple. The excitation frequency is 37 Hz. The velocities of hot and cold air are both 13 m.s^{-1} at the outlet of the air flow tubes. In any case, the measured time constants are longer during the heating phase than during the cooling one. This phenomenon corresponds to a greater magnitude of the convection coefficient (h). Table 2.5 presents convective time constants for the different thermocouple diameters, resulting from heating periods only and for two air flow velocities (13 m.s^{-1} and 23 m s^{-1}) and for a 5 to 72 Hz explored frequency bandwidth.

Table 2.5 Convective time constant τ_{cv} (ms) and bandwidth Δf (Hz) versus junction diameters. The thermocouple mechanical resistance is not sufficient for the flows with 13 m.s^{-1} and 23 m.s^{-1} air velocities

Junction diameter		Air velocity: 13 m.s^{-1}		Air velocity: 23 m.s^{-1}	
	d (µm)	τ_{cv} (ms)	Δf (Hz)	τ_{cv} (ms)	Δf (Hz)
S	0.5	–	–	–	–
	1.27	–	–	–	–
	5	2.9	55	2.2	72
K	12.7	15.2	10.5	8.5	18.7
	25	20	8	17	9.4
	250	32	5	25	6.4

One can notice that time constants decrease when increasing the flow velocity because of a larger surface over volume ratio exposed to the flow. Finally, even if the repeatability is good, such a calibration method remains however quite difficult to perform because the fragility of the sensor increases when the wires dimension decrease and the fluid flow increases.

b) Radiative calibration

This calibration method is based on a radiative excitation produced by a continuous argon laser [34, 35]. A set of two spherical lenses allows to locate the beam waist on the junction and an optical chopper generates a periodic modulation of the continuous laser beam. In order to avoid parasitic turbulences around the junction, the sensor is placed in a transparent enclosure (Figure 2.12.).

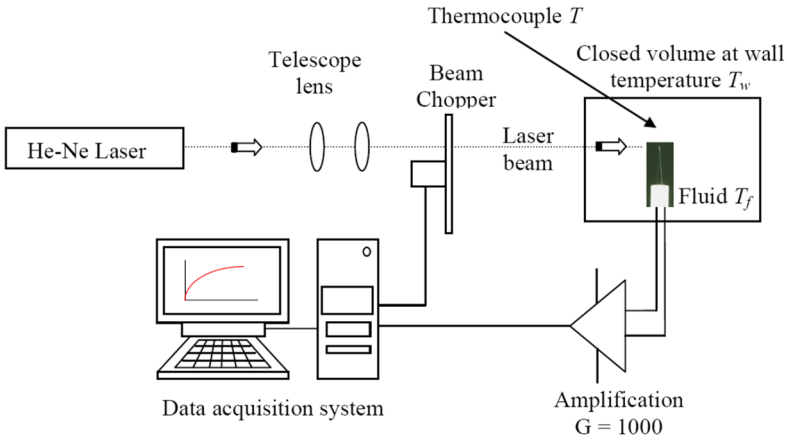

Figure 2.12. Radiative characterization setup

The signal obtained is close to a first order response which gives immediately the sensors dynamic performances. Time constants decreases as diameter and heat transfer (the laser power) increase (Figure 2.13.). This is consistent with the effect of an increasing value of the power density or a decreasing of the beam radius that both acts on the power to heated mass ratio. Table 2.6 presents the radiative time constant for all the thermocouple junction diameters and the explored frequency bandwidth is ranged from 5 to 2274 Hz.

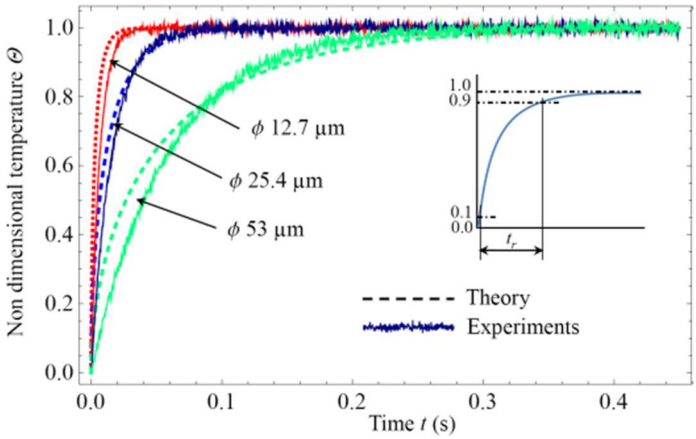

Figure 2.13.

Table 2.6 Radiative time constant τ_{rad} *(ms)* and bandwidth Δf *(Hz)* versus junction diameters

	Junction diameter d (µm)	Radiative time constant τ_{rad} (ms)	Bandwidth Δf (Hz)
S	0.5	0.07	2274
	1.27	0.18	884
	5	1.3	123
K	12.7	8.5	19
	25	34	5
	50	64.5	2.5

3.3. Microthermocouple designs

Different methods are used to design a thermocouple probe. It consists of a sensing element assembly, a protecting tube and terminations. Two dissimilar wires are joined at one end to form the measuring junction which can be a bare thermocouple element twisted and welded or butt welded. The protecting tube protects the sensing element assembly from the external atmosphere by a non ceramic insulation, a hard fired ceramic insulator or a sheeted compact ceramic insulator.

The thermocouple probe consists of two wires inserted in a ceramic double bore tube with length and external diameter depending on the experimentation. The wires are cut with a razor blade to produce a flat edge perpendicular to the axis. To realize the junction the thermocouple wires are connected to a bank of condensers (Figure 2.14.).

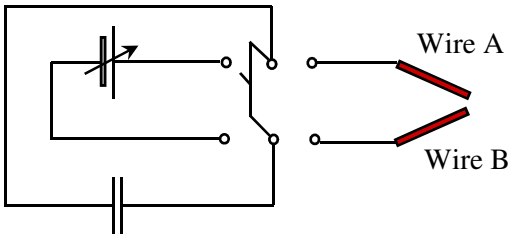

Figure 2.14. Thermocouple welding apparatus

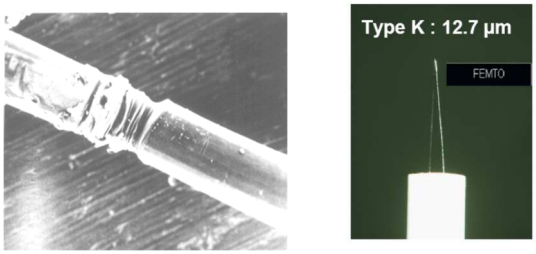

Figure 2.15. Thermocouple junction and probe

The two extremities are approached together in the same time and the beaded junctions are made by a sparking method. The energy release produced by the couple voltage-capacitance is sufficient to weld together the wires. One advantage of this technique is that the resulting junction diameter is not significantly greater than the wires one (Figure 2.15.). Except low mass and specific heat, another consequence is that the cross-sectional area of the wire itself can be used to calculate time constants. A drop of glue can be deposited at the tube extremity and pushed down around both wires to minimize the probe fragility.

4. Error introduced by the disturbance of the local temperature using thermocouples

4.1. Introduction

Whatever the selected measurement method, it is associated with parasitic effects which must be well-known. The resulting errors can be classified in two categories:

- the ones that are directly related to the thermometric phenomenon, they correspond to the inaccuracy on the measurement of thermometric quantities and to the parasitic effects attached to this phenomenon. It is not here the main topic, but they are not less important. We will quote simply for memory: singularities met in the laws of variation of electrical resistance due to structure modifications (allotropic transformations….), with chemical attacks… and for the thermoelectric circuits, the many parasitic effects such as e.m.f. induced, modifications of the thermoelectric force due to heterogeneities, modifications of structure, junctions nonspecific and not isotherms.

- the others, independently of the selected sensor are related to the fact that the interaction between thermometer, medium and environment causes a local disturbance of the temperature field therefore the local temperature is no more the one that exists before thermometric sensor settling.

In the following, we will present an error analysis and models to describe the local disturbance due to the presence of the sensors. These results come from various works performed at Laboratoire de Thermocinétique, Nantes (Bardon [36], Cassagne [37, 38])

4.2 Error analysis and model

4.2.1 Surface temperature measurement

The surface heat exchanges are modified by the presence of the sensor which does not have the same thermophysical and radiative properties and the same convective heat transfer as the medium to which it is applied. Therefore, a parasitic heat flow is transferred from the medium towards the sensor then from the sensor towards the environment as illustrated in figure 2.18. for surface temperature

measurement.

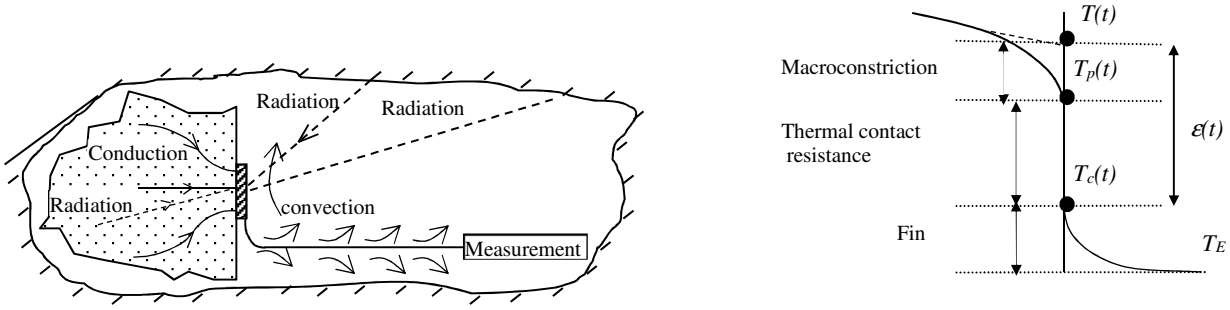

Figure 2.18. Surface temperature measurement

A heat generation or absorption closed to the sensor or to its connection can also occur. All these transfers induce, at the measurement location, a local temperature disturbance which can be either positive or negative according to the heat direction (going in or out). The temperature is no more T but T_p. Moreover, the sensor temperature is not usually equal to T_p because the imperfect contact conditions between sensor and medium involves a temperature discrepancy T_p-T_c which increases as the thermal contact resistance or the heat flux increases.

For an opaque medium, the following three effects are combined:

1. the effect of convergence of heat flux lines towards the sensor (macroconstriction effect),
2. the effect of thermal contact resistance which involves a temperature jump at the sensor/medium interface, and
3. the fin effect which corresponds to the heat transfer towards the outside (over the sensor and along its connection wires).

The measurement error is then:

$$\varepsilon(t) = T(t) - T_C(t) \qquad (2.33)$$

4.2.2. Temperature measurement within a volume

For temperature measurement within a volume, the analysis is similar to the previous one. The error independently of the chosen sensor depends on the fact that the sensor temperature almost never coincides with that of the small element which it replaces. The thermophysical characteristics of the sensors (λ, ρ, c) and its radiative properties are different from those of the medium.

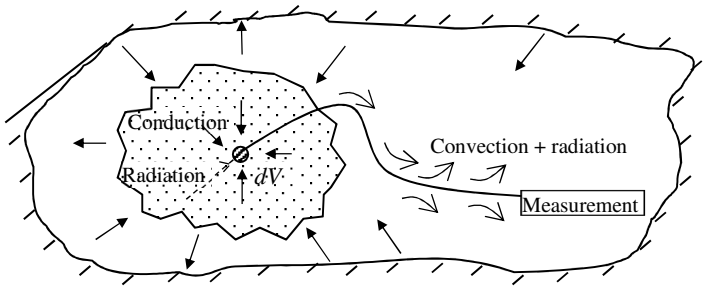

Figure 2.19. Temperature measurement within a volume

Heat transfer within the medium is modified by the presence of the sensor and similarly to surface temperature measurement, a local disturbance of the temperature field appears due to the heat transfer from the medium to the outside through the sensor. One still finds the three effects of: 1) convergence of the heat flux lines towards the sensor. 2) the thermal contact resistance effect 3) the fin effect. In addition the error is still: $\varepsilon(t) = T(t) - T_C(t)$

4.2.3. Error model

The study of the error related to the disturbance of the local temperature requires the solution of a multidimensional heat transfer problem with various possible configurations and boundary conditions. In this section, one will use relatively simple but very typical models that will clearly show the respective role of conduction within the medium, of nonperfect contact between sensor and medium and finally the heat exchanges towards the environment. Most of the conclusions could be extended to numerous other configurations.

We will suppose that the heat exchanges of the medium or of the thermometric connection with the environment can be represented by the heat transfer coefficient, h, and the outside equivalent temperature, T_E. It is known, for example, that for a surface which absorbs a heat flow F (radiation coming from a high temperature heat source) which exchanges by convection with a fluid at T_f temperature and by radiation with walls at temperature T_0 , one has:

$$h = h_c + h_r \tag{2.34}$$

$$T_E = \frac{h_c T_f + h_r T_0 F}{h} \tag{2.35}$$

where h_c is the convection heat transfer coefficient, $h_r = 4A\sigma T_m^3$ the radiation coefficient (A is a coefficient which depends on the emissivity and of the relative location of surfaces between which the radiative heat exchange occurs, T_m is an intermediate temperature between T_0 and that of the surface).

4.2.3.1. Steady state surface temperature measurement of an opaque medium

One will investigate surface temperature measurement on an opaque medium of thermal conductivity λ with a simplified sensor having the shape of a rod perpendicular to the surface (figure 2.20.). Far from the sensor, the medium is at the constant temperature T. The surface of the medium is assumed adiabatic except at the contact area S with the sensor.

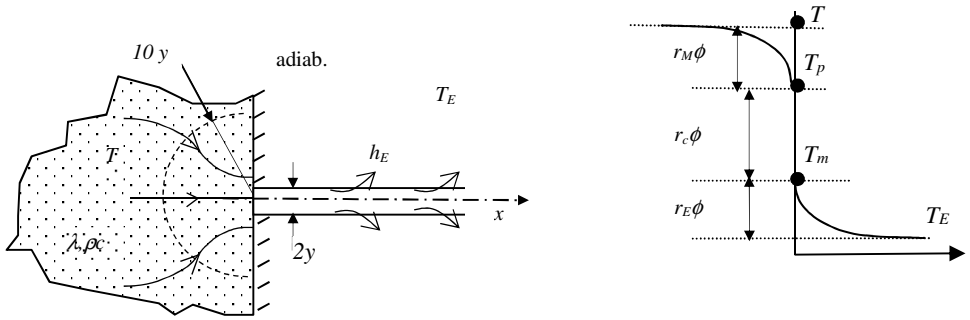

Figure 2.20. Steady state configuration

The three following effects occur due to heat leakage through the sensor towards the outside:

a) The convergence effect: it results from the relation between true temperature and disturbed temperature:

$$T - Tp = r_M \phi \qquad (2.36)$$

where r_M is a macroconstriction resistance and ϕ the parasitic heat flux. With a 3D heat transfer calculation, one can show that $r_M \cong \frac{0{,}4789}{\lambda\sqrt{s}}$ and for a circular surface of radius ρ: $r_M = \frac{1}{4\rho_O\lambda}$.

It is also shown that 96% of the $T - T_p$ temperature drop is within a hemisphere of center 0 and radius 10ρ or $5{,}7\sqrt{s}$.

b) *The contact resistance effect*: responsible of the $T_p - T_c$ temperature drop, it is expressed by:

$$T_p - T_c = r_c \phi \qquad (2.37)$$

where r_c represents the thermal contact resistance for the surface S (if R_c is the resistance per unit of surface: $r_c=R_c/S$). This effect is related to the imperfection of the contact which results from the irregularities of surfaces. The contact between two solid media is carried out only in some areas (~ 1% of the apparent surface) between which remains an interstitial medium.

c) *The fin effect:* It is responsible for the heat transfer between the connection of the sensor and the environment. Whatever the assumed shape of the connection (rods with uniform or variable section) the heat flux ϕ transferred from the face at $x = 0$ to the environment is linked to the temperature difference (between T_c at x = 0 and the equivalent outside temperature T_E) defined by:

$$T_c - T_E = R_E \phi \qquad (2.38)$$

where T_c is the temperature at $x = 0$, T_E the equivalent outside temperature and R_E the total thermal resistance between the face x = 0 and the environment. It depends particularly on the geometry, the heat transfer coefficient and the thermal conductivity λ_E of this external connection:

$R_E = 1/(\pi y_E\sqrt{2h_E\lambda_E y_E})$ for a thermocouple assumed as a rod of radius y_E . From relations (2.36, 2.37 and 2.38), one can deduce the heat flux: $\phi = \frac{T - T_E}{r_M + r_c + r_E}$ and the measurement error:

$$\delta T = K\,(T - T_E) \qquad (2.39)$$

with

$$K = \frac{1}{1 + \frac{r_E}{r_c + r_M}} \qquad (2.40)$$

The error is thus proportional to the measured and equivalent outside temperatures difference (T-T_E), the "error coefficient" K is all the more small as the sum of resistances of macro-constriction r_M and contact r_c will be small compared to the external resistance r_E. Therefore, it results that:

- For measurements on a high thermal conductivity medium (metal) , $r_M << r_c$, the thermal contact conditions determines the errors
- For measurements on a low dielectric material, $r_M >> r_c$, the effect of macroconstriction determines the error.
- The roles of r_E and T_E are finally very important. One needs the largest possible r_E and T_E nearest to T (probe with heat flux compensation). It is worth to focus one's attention to the heat flux ϕ_E generated on the surface of the connection wire. If T_E can become much higher than T, the error is changed by sign and is of great amplitude: it is necessary to avoid the external

radiation of source on the connection. These conclusions, found for the temperature measurement on an opaque medium and for a simplified configuration of a sensor having the shape of a rod perpendicular to surface, remain valid with slight differences for real configurations.

4.2.3.2 Transient surface temperature measurement of an opaque medium

For a fast sudden contact between an opaque medium and a sensor assumed as a rod and perpendicular to its surface, the error becomes a function of time: $\varepsilon(t) = K(t)\,[T(t) - T_E]$. It remains proportional to the temperature difference: $T(t) - T_E$

The coefficient $K(t)$ is maximum for $t \rightarrow 0$ and decreases for higher t values. For $t \rightarrow \infty$, one has: $K(T) \rightarrow K(\infty)$ which is obtained for a steady state. The contact condition between sensor and medium is of great importance:

- If $r_c \neq 0$, $K(0)=1$, the error is about 100% at $t=0$ and decreases all the more the contact between sensor and medium is good.
- If $r_c = 0$ (perfect contact), the initial error is smaller:
  $K(0) = \frac{b}{b+b_E} < 1$ where $b = \sqrt{\lambda \rho c}$ and $b_E = \sqrt{\lambda_E \rho_E c_E}$ are the medium and connection effusivities**.**

One can characterize the thermal inertia by the time response x%, such as (figure 2.21.): $\frac{K(t_x) - K(\infty)}{K(0) - K(\infty)} = x$

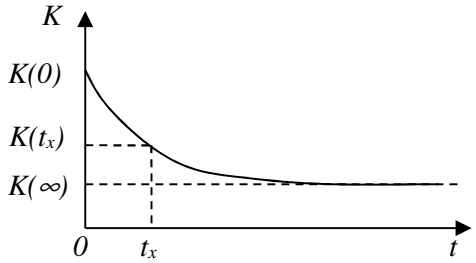

Figure 2.21.

For the same sensor, t_x depends strongly on the characteristics of the medium and on the connection medium/sensor/environment. For a conducting medium, t_x depends strongly on r_c which appears as the main factor that determines the sensor inertia. t_x decreases when r_c decreases. It is the same thing if the diameter of the connections is reduced.

For fast transient evolutions, it is worth to weld wires on the surface, so that $r_c \rightarrow 0$, and to use wires as thin as possible. In this case $(r_c \sim 0)$, the thermal inertia t_x is primarily determined by the establishment time t^* of the macro-constriction phenomena within the medium. In practice, this phenomenon remains extremely localized within the immediate vicinity of the sensor (hemisphere of radius $10y$), one can deduce an order of magnitude for t^* by considering the characteristic time $t^* \approx 100y^2/a$ associated to this hemisphere. One can consider that, at this time t^*, constriction is established at 97%. One can thus consider that $t_x \approx t^* \approx 100y^2/a$. For temperature with insulating mediums, r_c does not have any effect but t_x is much higher. For a transient evolution with a characteristic time t_c, it is worth to choose a sensor

for which $t_x << t_c$. In this case, as soon as $t > t_x$, the error will reach, at every moment, its minimal asymptotic value and the steady error model (K_∞) could be applied.

4.2.3.3. Temperature measurement within a volume

In this case, the connection wires usually do not follow an isothermal path on a sufficient length, therefore heat leakage through the sensors occurs. Measurements within a volume are in general much easier than on a surface, and errors are usually smaller. However, their analysis is more difficult to carry out especially because of the interaction between the connection wire and the medium. In addition, a cavity has to be realized for sensor introduction.

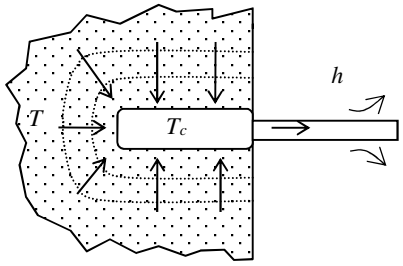

Figure 2.22. Temperature measurement with a cylindrical sensor inside the medium

Therefore, the cavity and the sensors don't match exactly, so there exists, between them, some residual space filled with air, grease, glue… which introduces a thermal resistance between sensor and medium. The measurement errors introduced by these phenomena are qualitatively rather similar to those described for surface temperature measurements. Lastly, for long enough isothermal path, heat transfer between sensor and environment is negligible, the differences between thermophysical characteristics (conductivity, heat capacity) of the medium, of the probe or the wire of connection or residual space, introduce a localized disturbance of the thermal field, and a measurement error remains, but this one is much smaller. An example is provided in figure 2.22.

With this configuration, the previous error model (2.39 and 2.40) is still valid, the value of r_c and r_M being different. If we consider that the sensitive element of the sensor with a length L, and a radius y, which recovers its surface S, is isothermal and that its temperature is T_c (figure 2.22.). The contact between the probe and the medium is supposed to be imperfect, therefore for the whole surface of the sensor, the thermal contact resistance r_c is: $r_c = R_c/S$ with $S=2\pi yL$. If $T_E \neq T$, a heat flux occurs between the medium and the environment. The temperature field is modified. In this case, the thermal constriction resistance is expressed by: $r_M = \frac{1}{2\pi\lambda\ell} Log \frac{2\ell}{y}$ with $\ell >>$ y.

4.3. Practical consequence and examples, semi-intrinsic thermocouples

4.3.1. Practical consequences

The steady state error model for the simple configuration allows some important features, most of them being valid for other configurations:

1) first of all even for perfect contact $r_c = 0$, there is an error which depends on the ratio r_M / r_E.
2) if the medium is a *high thermal conductivity* material, the macro-constriction r_M will be usually small relatively to r_c and the error will be especially determined by r_c. Thus, one must take care

that r_c is small and remains stable. The contact pressure has to be high and constant, surface has to be plane without waviness, the interstitial medium with the highest possible thermal conductivity (welding, grease…). In addition, one should avoid oxide films as well as mechanical shocks and vibrations which can modify considerably r_c and consequently the measurement error.

3) For measurements on *an insulator*, r_M is large, usually much higher than r_c. Thus, the macro-convergence effect is the main factor in the measurement error and one can reduce it by increasing the radius of the sensitive element without increasing the section of the connections (figure 2.23.). A contact disc of high thermal conductivity material will be used.

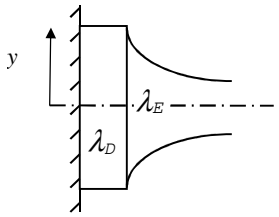

Figure 2.23.

4) Whatever the type of measurement, the fin resistance r_E should be as high as possible. The transversal area, the conductivity, the heat transfer coefficient has to be chosen the smallest possible. One also should have low emissivity surface, connection protected from high temperature fluids movements or radiation, T_E being modified in those situations. One should note that having an insulating layer on the metallic wire of the thermocouple can increase the side heat transfer and therefore the measurement error.
5) Finally, the error is all the more small as T_E is close to the temperature to measure T. It changes with T_E. At the price of a technological complication, one can add an external heat source on the connection so that its temperature T_E is controlled in order to stay as close as possible as T. In this case, one reduces considerably the heat transfer and consequently the error of measurement. This principle is well known as "compensated heat flux sensors". However, for correct measurement, the thermal resistance r_E should stay high in order to prevent the compensation heating from disturbing the temperature field in the medium.

4.3.2. Application -for steady state temperature measurement for a thermocouple with and without a contact disc

The two thermocouple wires are considered as an unique rod with a radius y_B = 0.5 mm, an infinite length, an average thermal conductivity λ_B = 15 $W.m^{-1}.K^{-1}$ and a heat transfer coefficient $h_B = 5\ W.m^{-2}K^{-1}$.

The fin thermal resistance is: $r_B = \frac{1}{\pi y_B \sqrt{2h_B y_B \lambda_B}}$ (rod approximation)

Thus, the connection resistance is:

- $r_E = r_B$ without contact disc,
- $r_E \approx r_B + \frac{1}{4 y_B \lambda_D}$ with contact disc

($\frac{1}{4 y_B \lambda_D}$ is the resistance due to heat flux convergence from y to y_B inside the sensor).

Table 2.9. provides the values of r_M, r_c, r_E and K and for various λ_D with and without disc ($y=y_B=10\ mm$, $\lambda_D = \lambda_B$) and for different values of R_c per unit of area:

Table 2.9. Effect of medium thermal conductivity and of the disc on r_M, r_c, r_E and K

	Low thermal conductivity $\lambda=10^{-1}\ W.m^{-1}.K^{-1}$		High thermal conductivity $\lambda=100\ W.m^{-1}.K^{-1}$	
	without disc	with disc	without disc	with disc
$r_M (K.W^{-1})$	5000	250	5	0.25
$R_C (K.W^{-1}m^2)$	10^{-3}	10^{-3}	10^{-4}	10^{-4}
$r_C (K.W^{-1})$	1270	3,18	125	0,31
$r_E (K.W^{-1})$	1700	1733	1700	1733
K	0.786	0.127	0.072	0.0003

5. Temperature measurement with semi-intrinsic thermocouple

In this device, one uses the medium M itself (presumately electrically conducting) as one item of the thermocouple (figure 2.24.). Compared to a traditional sensor, this device has several advantages:

- it has only one connection wire instead of two, thus heat leakage is reduced and the thermal resistance r_E is twice larger.
- the measured temperature T_μ is intermediate between T_p and T_c (figure 2.24.)

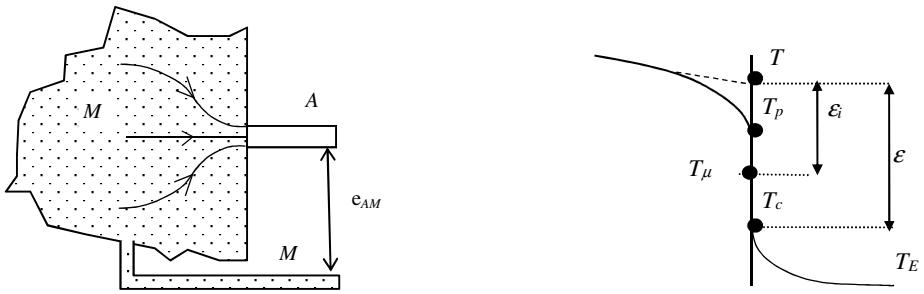

Figure 2.24. Semi intrinsic thermocouple

For times $t > t_c$ (time constant), T_μ is such that: $$\frac{T_p - T_\mu}{T_\mu - T_c} = \frac{\lambda_A}{\lambda_M} \qquad (2.41)$$

The error $\varepsilon_i = T - T_\mu$ is thus lower and the contact resistance effect is partly cancelled. For steady state, the error is such that:

$$\varepsilon_i = K_i \left(T - T_E\right) \qquad (2.42)$$

With $$K_i = \frac{r_M + r_c \dfrac{\lambda_A}{\lambda_A + \lambda_M}}{r_M + r_c + r_E} \qquad (2.43)$$

This error is considerably lower than with a traditional thermocouple (2 to 5 times) and this as much more as the wire thermal conductivity λ_A is small compared to λ_M. In transient mode, error and thermal inertia are greatly reduced (Bardon [36], Cassagne [37]). However, the calibration of the semi-intrinsic thermocouple is almost always required. It is usually performed by comparison with a traditional thermocouple.

6. Heat flux measurement: direct and in direct methods

6.1. Direct measurement

6.1.1. Heat flux sensor with gradient (Ravaltera [39])

The principle of this heat flux measurement consists in directly applying the Fourier's law by measuring a temperature difference within the wall itself (intrinsic method) or by covering it with an additional wall (heat flux sensor-HFS-). The surface characteristics of this HFS should be close to those of the wall. The wall of the HFS can be homogeneous (the temperature difference is measured between its two main faces -normal gradient heat flux sensor- figure 2.25.-) or it can be heterogeneous creating heterogeneous temperature that is measured (tangential gradient heat flux sensor – figure 2.26.-).

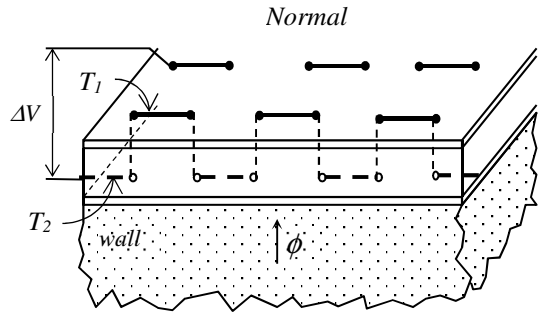

Figure 2.25.

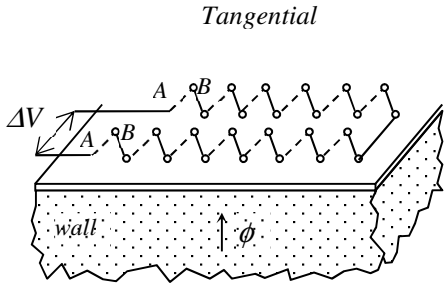

Figure 2.26.

The installation of such HFS on a wall, more or less disturbs the heat flux which crosses it. All must be done so that internal and contact thermal resistances are minimal. In these devices, the measurement of the temperature difference is performed using several thin film thermocouples or thermoresistances. These HFS can work whatever the heat flux direction in steady state or for slowly variable temperature.

Table 2-10 shows a list of commercially available normal or tangential heat flux sensors

Table 2-10 : Main characteristics of available commercial normal and tangential heat flux sensors

Heat flux sensor	**N /T**	**Dim [mm]**	**T_{max}** [°C]	**Sensitivity [μV/(W.m^{-2})]**	**Thick [mm]**	**R_{th} x 10^3 [m^{2}K/W]**	**Response time [s]**	**Accuracy Heat flux [%]**
Hioki	N	10 x10	150	13	0.28	1.4		
RdF/Omega	N	11.93 x25.4	150	1.0	0.125	0.88	0.09	~8-10
RdF/omega	N	11.93 x25.4	150	3.48	0.33	2.1	0.4	~8-10
Wuntronic FM120	N	7.4 x10.7	150	2.64	1.5	4.75	3	5 (Fab)
Flux Teq	N	25.4 x25.4	120	0.8	0.38	0.65	0.6	
GreenTEG gskin	N	10 x10	150	50	0.5	0.35	0.2/0.7	3
Captec	T	10 x10	120	3 à 5		1	0.3	~8-12

N: normal; T: tangential

6.1.2. Inertia heat flux sensor and heat flux sensor with electric dissipation (zero method)
Inertia heat flux sensors works only for variable temperature and if the heat flux is received by the wall. The HFS replaces a piece of the wall and is isolated from this one. Its surface characteristics are identical to those of the wall. The HFS temperature increase is proportional to the absorb heat flux and inversely proportional to its capacity (figure 2.27.). The choice of this one is very important because it determines the measurement sensitivity.

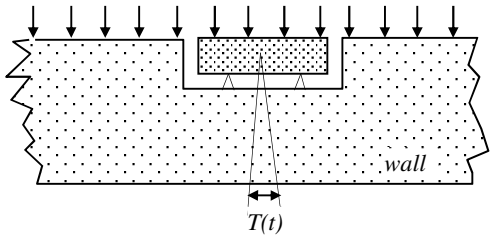

Figure 2.27.

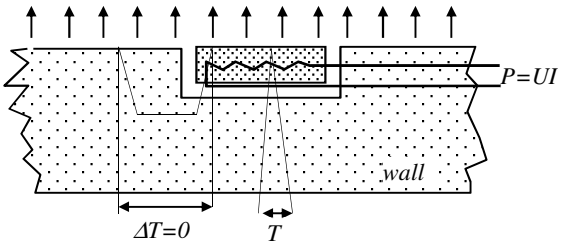

Figure 2.28.

The principle of this HFS with electric dissipation consists in substituting a piece of the wall at its surface with a small heating part insulated towards the wall (fig. 2.28.). The electric heating output is adjusted so that the surface temperature of the wall and of the heating part are equal (*ΔT=0*). Thus, the dissipated electric flux is equal to the heat flux which leaves the wall in its immediate vicinity. This HFS works only for heat flux leaving the wall and for steady state or slowly variable temperature.

6.1.3. Enthalpic heat flux sensor
They are used to measure the heat flux coming from the outside. The HFS replaces an element of surface of the wall and is insulated from this one (figure 2.29.). An initially temperaturecontrolled fluid circulation is heated by the heat flux which induces an enthalpic flow rate. For a correct measurement, the fluid temperature must be adjusted so that wall and HFS temperatures are almost equal. This condition is not always realized and can be an important source of error. The choice of the heat-storage capacity of the fluid also is important.

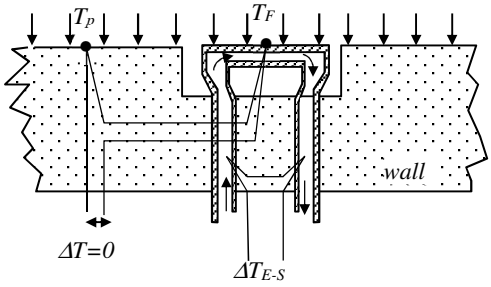

Figure 2.29.

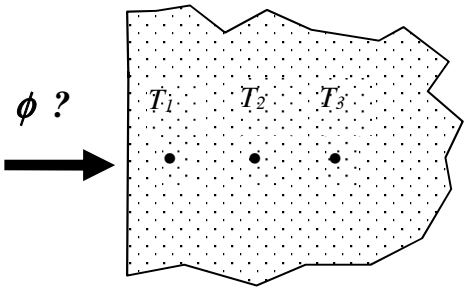

Figure 2.30.

6.1.4. Indirect measurement

One can obtained the surface characteristics (temperature T, heat flux φ) from measurements realized within the medium and using inverse methods (figure 2.30.). This procedure involves solution of ill-posed problems. Indeed, one cannot insure a solution, its uniqueness or stability. To solve such difficulties, the technique consists in replacing the ill posed problem by a well posed approximate problem. The solution is found by minimizing a norm of least square type. A heat transfer model (analytical or numerical) is required to solve the direct problem at each optimization step. These methods require significant developments (Beck [40], Alifanov [41], Ozisik [42], Jarny [43]). They will not be presented here. We will just underline that the solution of the inverse problem allows to compute the temperature residuals between final and measured temperatures. These residuals are of great importance because they allow to check the validity of the chosen heat transfer model. If no signature is observed (the residuals are purely random) the model is correct, otherwise the model should be improved.

With regard to the theoretical aspects of the instrumentation, Bourouga [44] has proposed criteria for correct locations of thermocouples to obtain unbiased results and also to optimize the experiment for wall heat flux or temperature estimation.

7. Conclusion

Accurate temperature measurement is not an easy task. Errors depend on thermosensitive phenomena and also according to the sensors which can create local temperature disturbance and therefore bias. Very often, this latter error is ignored. In this lecture dedicated to contact temperature measurement, one has tried to provide to the readers the know-how in various situations (temperature measurement in fluids or opaque medium) in order to perform the best temperature measurements as possible.

8. References

[1] Seebeck, T.J. 1823. Magnetische polarisation der metalle und erze durch temperatur-differenz, *Abh. K. Akad. Wiss.* Berlin, 265

[2] Peltier, J. C. A. 1834. *Annales de Chimie et de Physique* 56: 371-470.

[3] Thomson, W. 1848. On an Absolute Thermometric Scale founded on Carnot's Theory of the Motive Power of Heat, and calculated from Regnault's Observations, *Philosophical Magazine* 33:313-317.

[4] Rathakrishnan, E. 2007. *Instrumentation, Measurements and Experiments in Fluids*, CRC Press.

[5] Devin E. 1997. Couples thermoélectriques, données numériques d'emploi, *Techniques de l'Ingénieur*, tome R2594 :1-26.

[6] Forney, L.J. and Meeks, E.L., Ma, J., Fralick, G.C. 1993. Measurement of frequency response in short thermocouple wires, *Rev. Sci. Intrum.* 64 (5) :1280-1286.

[7] Yule, A.J. and Taylor, D.S., Chigier, N.A. 1978. On-line digital compensation and processing of thermocouples signals for temperature measurements in turbulent flames, *AIAA 16th Aerospace Sciences Meeting,* 78–80.
[8] Lenz, W. and Günther, R. 1980. Measurement of fluctuating temperature in a free-jet diffusion flame, *Comb. and Flame* 37:63-70.
[9] Lockwood, F.C. and Moneib, H.A. 1980. Fluctuating temperature measurements in a heated round free jet, *Comb. Sci. and Technology* 22:63-81.
[10] Voisin, P. and Thiery, L., Brom, G. 1999. Exploration of the atmospheric lower layer thermal turbulences by means of microthermocouples, *E.P.J. App. Phys.* 7(2):177-187
[11] Pitts, W.M. and Braun, E.B., Peacock, R.D., Mitler H.E. et al. 1998. Temperature uncertainties for bare-bead and aspirated thermocouple measurements in fire environnement*s,* in Proceedings of the 14th Meeting of the United States Japan conference on Development of Natural Resources (UJNR) Panel on Fire Research and Safety, May, Japan.
[12] Blevins, L.G. Pitts, W.M. 1999. Modeling of bare and aspirated thermocouples in compartment fires, *Fire Safety J.* 33(4):239-259.
[13] Santoni, P-A. and Marcelli, T., Leoni, E. 2002. Measurement of fluctuating temperatures in a continuous flame spreading across a fuel bed using a double thermocouple probe. *Combustion and Flame* 131(1-2):47-58.
[14] Rakopoulos, C. D. and Rakopoulos, D.C., Mavropoulos, G.C., Giakoumis, E.G. 2004. Experimental and theoretical study of the short term response temperature transients in the cylinder walls of a diesel engine at various operating conditions, *Appl. Therm. Eng.* 24(5-6):679-702.
[15] Bardon, J.P. and Raynaud, M., Scudeller, Y. 1995. Mesures par contact des températures de surface, *Rev. Gén. Therm.* 34(HS95):15-35.
[16] Paranthoen, L. and Lecordier, J.C. 1996. Mesures de température dans les écoulements turbulents, *Rev. Gén. Therm.* 35 :283-308.
[17] Olivari, D. and M. Carbonaro. 1994. *Hot wire measurements. Measurements techniques in fluid dynamics. an introduction*, Von Karman Institut for Fluid Dynamics, *Annual Lecture Series*, vol. 1:183-218.
[18] Million, F., Parenthoën, P., Trinite, M. 1978. Influence des échanges thermiques entre le capteur et ses supports sur la mesure des fluctuations de température dans un écoulement turbulent, *Int. J. Heat Mass Transfer* 21:1-6.
[19] Bradley, D. and Mathews, K. 1968. Measurement of high gas temperature with fine wire thermocouple. J. Mech. Engn. Sci. 10(4):299-305.
[20] Collis, D.C. and Williams, M.J. 1959. Two dimensional convection from heated wires at low Reynolds numbers. *J. of Fluid Mech.* 6:357-384.
[21] Knudsen, J.G. and D.L. Katz. 1958. *Fluid dynamics and heat transfer*, Mc Graw-Hill Book Co., New-York.
[22] Van der Hegg Zijnen, B.G. 1956. Modified correlation formulae for the heat transfer by natural and by forced convection from horizontal cylinders. *Appl. Sci. Res.* A(6):129-140.
[23] Mac Adams, W.H. 1956. *Heat transmission*, Mc Graw-Hill Book Co., New-York.
[24] Eckert, E. R. and Soehngen, E. 1952. Distribution of heat transfer coefficients around circular cylinders, Reynolds numbers from 20 to 500, *Trans. ASME*, *J. Heat Transfer*, 74:343-347.
[25] Scadron, M.D. and Warshawski, I. 1952. Experimental determination of time constants and Nusselt numbers for bare-wire thermocouples in high velocity air streams and analytic approximation of conduction and radiation errors, NACA, T.N., 2599.
[26] Tarnopolski, M.and Seginer, I. 1999. Leaf temperature error from heat conduction along the wires, *Agr. For. Meteo.*, 93(3):185-190.
[27] Bailly, Y. 1998. Analyse expérimentale des champs acoustiques par méthodes optiques et microcapteurs de température et de pression, Ph. D. diss, University of Franche-Comté, France.

[28] Fralick, G.C. and Forney, L.J. 1993. Frequency response of a supported thermocouple wire: effects of axial conduction, *Rev. Sci. Intrum.* 64(11):3236-3244.
[29] Sbaibi, H. 1987. Modélisation et étude expérimentale de capteurs thermiques, Ph. D. diss, University of Rouen, France.
[30] Singh, B.S. and Dybbs, A. 1976. Error in temperature measurements due to conduction along the sensor leads, *J. Heat Transfer* 491:491-495.
[31] Kramers, H. 1946. Heat transfer from spheres to flowing media, *Physica* 12:61-80.
[32] King, L.V. 1914. On the Convection of Heat from Small Cylinders in a Stream of Fluid, *Phil. Trans. of Roy. Soc. (London),* Ser. A., 214(14):373-432.
[33] Hilaire, C. and Filtopoulos, E., Trinite, M. 1991. Mesure de température dans les flammes turbulentes. Développement du traitement numérique du signal d'un couple thermoélectrique. *Rev. Gén. Therm.* 354/355 :367-374.
[34] Castellini, P. and Rossi, G.L. 1996. Dynamic characterization of temperature sensors by laser axcitation, *Rev. Sci. Instrum.* 67(7):2595-2601.
[35] Hostache, G. and Prenel J.P., Porcar, R. 1986. Couples thermoélectriques à définition spatiotemporelle fine. Réalisation. Réponse impulsionnelle de microjonctions cylindriques. *Rev. Gén. Therm.* 299 :539-543.
[36] Bardon J P 2001 « *Mesure de température et de flux de chaleur par des méthodes par contact*», Lecture c2b, Ecole d'Hiver METTI , Odeillo, 25-30 jan 1999, Vol.1, (Perpignan: Presse Univ).
[37] Cassagne B, Bardon J P and Beck J V 1986 «*Theoretical and experimental analysis of two surface thermocouple*», Int. Heat Transfer Conf., San Fransisco.
[38] Cassagne B, Kirsch G and Bardon JP 1980 *Int. J. Heat Transfer* **23** 1207-1217
[39] Ravaltera G, Cornet M, Duthoit B and Thery P 1982 *Revue Phys. Appl.*. **17** 4 177-185
[40] Beck J V, Blackwell B and StClair C.A., 1985 Inverse heat conduction (New York: Wiley)
[41] Alifanov O.M 1990 Inverse heat transfer problems (Springer)
[42] Ozisik N 1993 Heat conduction 2d ed.. (New York: Wiley)
[43] Jarny Y, Ozisik M.N and Bardon JP 1991 Int J Heat Mass Transfer 34,11, 2911-2919
[44] Bourouga B., Goizet V and Bardon J P 2000 Int. J. Therm. Sci. 39 96-109